

Nucleosynthesis in massive stars revisited

T. Rauscher^{ab*}, A. Heger^b, R. D. Hoffman^c, and S. E. Woosley^b

^a Department of Physics and Astronomy, University of Basel, Basel, Switzerland

^b Department of Astronomy and Astrophysics, UC Santa Cruz, Santa Cruz, CA, USA

^c Lawrence Livermore National Laboratory, Livermore, CA, USA

We have performed the first calculations to follow the evolution of all stable nuclei and their radioactive progenitors in a finely-zoned stellar model computed from the onset of central hydrogen burning through explosion as a Type II supernova. Calculations were done for $15 M_{\odot}$, $20 M_{\odot}$, and $25 M_{\odot}$ Pop I stars using the most recently available set of experimental and theoretical nuclear data, revised opacity tables, and taking into account mass loss due to stellar winds. Here results are presented for one $15 M_{\odot}$ model.

1. INTRODUCTION

Stars above $\sim 10 M_{\odot}$ are responsible for producing most of the oxygen and heavier elements found in nature. Numerous studies have been devoted to the evolution of such stars and their nucleosynthetic yields, e.g., [1,2]. However, our knowledge of both the input data and the physical processes affecting the evolution of these stars has improved dramatically in recent years. Thus, it became worthwhile to improve on and considerably extend the previous investigations of pre- and post-collapse evolution and nucleosynthesis. We present the first calculation to determine, self-consistently, the complete synthesis of all stable nuclides in any model for a massive star. Due to the limited space, in this report we mainly focus on giving an outline of our investigations. For further details on the calculations and results the reader is referred to the full papers [3,4].

2. REACTION NETWORK

We employed a nuclear reaction network of unprecedented size in full stellar evolution calculations. The network used by [1] (WW95), large in its day, was limited to 200 nuclides and extended only up to germanium. Studies using reaction networks of over 5000 nuclides have been carried out for single zones or regions of stars, especially to obtain the r-process, e.g., [5–7], but “kilo-nuclide” studies of nucleosynthesis in complete stellar models (typically of 1000 zones each) have been hitherto lacking. Similar to WW95, nucleosynthesis was followed by co-processing the stellar model throughout its evolution using the extended nuclear reaction network. From hydrogen ignition through central helium depletion a 617 nuclide network was employed that included all elements up to

*Supported by a PROFIL professorship of the Swiss SNF.

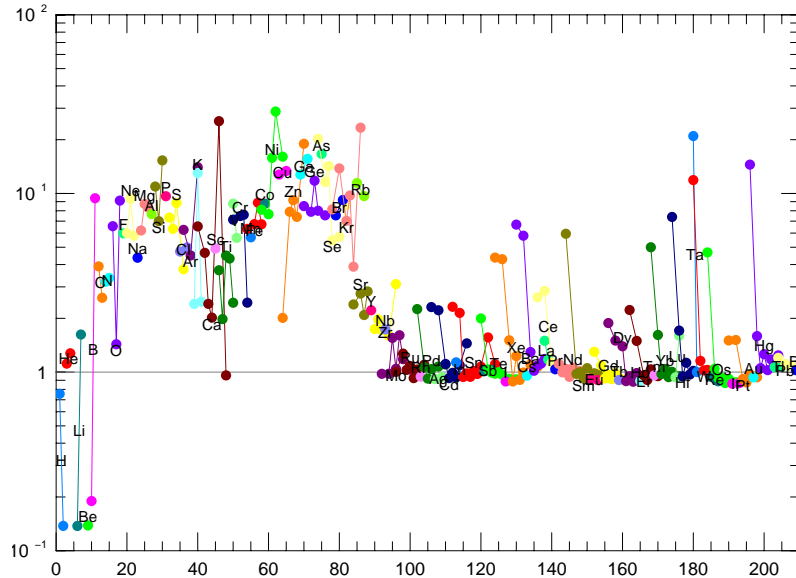


Figure 1. Production factors in the ejecta of a $15 M_{\odot}$ star relative to solar abundance vs. nuclear mass number.

polonium, adequate to follow the s-process. Just prior to central carbon ignition, we switched to a network containing 1482 nuclides. That network incorporated more neutron-rich isotopes to follow the high neutron fluxes in carbon (shell) burning and was also slightly extended on the proton-rich side to follow the γ -process [8,9]. The nucleosynthesis during the supernova explosion itself was followed in each zone using a 2437 nuclide network including additional proton-rich isotopes to better follow the γ -process in the neon-oxygen core, and also many additional neutron-rich isotopes to follow the n-process expected during supernova shock front passage through the helium shell. Here we will ignore the nucleosynthesis that occurs in the neutrino wind which may be the principal site of the r-process because its thermodynamic properties continue to be poorly understood.

3. INPUT PHYSICS

Our calculations were performed using the stellar evolution code KEPLER [1] with several modifications relative to WW95 (mass loss due to stellar winds [10], improved adaptive network) and updates (OPAL95 opacity tables [11], neutrino loss rates [12]). We generated a new library of experimental and theoretical reaction rates. As the basis of our reaction rate set we used statistical model calculations obtained with the NON-SMOKER code [13,14]. A library of theoretical reaction rates calculated with this code and fitted to an analytical function — ready to be incorporated into stellar model codes — was published recently [14]. It includes rates for all possible targets from proton to neutron dripline and between Ne and Bi, thus being the most extensive published library of theoretical reaction rates to date. For the network described here we utilized the rates based on the FRDM set. This was supplemented with experimental neutron

capture rates along the line of stability [15]. Experimental (α, γ) rates were implemented for ^{70}Ge [16] and ^{144}Sm [17]. The derived $\alpha+^{70}\text{Ge}$ and $\alpha+^{144}\text{Sm}$ potentials were also utilized to recalculate the transfer reactions involving these potentials. For the important rates for α -capture reactions on self-conjugated ($N = Z$) nuclides, a new semi-empirical rate determination was implemented [18]. For comparison, we used different sets of experimental and theoretical rates for elements below neon: WW95, Ref. [19], and NACRE [20]. Experimental β^- , β^+ , and α -decay rates were taken from [21] and theoretical β^- and β^+ rates from [22]. As a special case, we implemented a temperature-dependent ^{180}Ta decay [23]. For $A \leq 40$ we also included recent theoretical weak rates [24]. We did not follow the ν -process for nuclides with Z or N larger than 40. The supernova explosion was simulated, as in [1], by an inward–outward moving piston resulting in a total kinetic energy of the ejecta at infinity of 1.2×10^{51} erg. The final mass cut outside the piston is determined self-consistently from the hydrodynamic calculation.

4. RESULTS AND DISCUSSION

Here we only summarize the important results for one $15 M_{\odot}$ Pop I star. The production factors of this non-rotating model are shown in Fig. 1 as an example of our results. The model included mass loss and the rate set of [19] below Ne. Note, however, that though this mass is a numerically typical case of a Type II or Ib supernova, the average nucleosynthetic yield of massive stars is the result of populations of different stars each of which has its own peculiar yields which must be combined to result in a solar-like abundance pattern. Other stars and rate sets will be discussed in [3].

4.1. Stellar structure

The revision of the opacity table and the introduction of mass loss generally leads to smaller helium core sizes which tend to also decrease the mass of the carbon-oxygen and the silicon core. Note, however, that the absolute values of these core masses depend on the uncertainties, in particular, of the mixing processes in the stellar interior, such as semiconvection, overshooting, and rotation.

The change in the weak rates [24], important after central oxygen burning, leads to a 2–3% higher electron fraction per nucleon, Y_e , at the time of core collapse in the center of the star and the “deleptonized core” tends to comprise less mass [4]. More important for the core collapse supernova mechanism might be the 30–50% higher densities of the new models between the region of $m = 1.5 - 2 M_{\odot}$ [4], which may result in a correspondingly higher ram-pressure of the infalling matter.

4.2. Intermediate and heavy element nucleosynthesis

A strong secondary s-process contribution appears between iron and a mass number of $A = 90$. Above $A = 100$ the s-process in our $15 M_{\odot}$ star is very weak, but it becomes notably stronger in stars with more massive helium cores that perform helium burning at higher entropies. Furthermore, the strength of the s-process is found to be very sensitive to the (α, n) – (α, γ) rates and branching on ^{22}Ne which is experimentally not well determined (see also [25]). Second only to the well-known strong dependence of the stellar structure on the $^{12}\text{C}(\alpha, \gamma)$ rate, it becomes another important candidate for further laboratory study.

The proton-rich heavy isotopes above $A = 123$ can be well produced by the γ -process

occurring during implosive and explosive oxygen and neon burning. The proton-rich isotopes around $A = 160$ and those between $A = 100$ and $A = 123$, however, are under-produced by a factor of 3 to 4 with respect to ^{16}O . The isotope ^{180}Ta seems to show a strong overproduction by the γ -process. However, in the figure only the totally produced ^{180}Ta is shown. The surviving yield can be brought down to a more consistent production level by accounting for the distribution between ground and isomeric states [3].

The expected r- or n-process production by the supernova shock front passing through the base of the helium shell is not significant in any of our model stars, not even at $A = 130$. We observed some redistribution of isotopes at the base of the helium shell around $A = 123$ but this did not show the characteristics of a typical r-process nor was it important compared to the total yield of the star.

Summarizing, we have presented the first calculation to follow the complete s-process through all phases of stellar evolution and the γ -process in the whole star through the presupernova stage and subsequent supernova explosion. This research was supported, in part, by DOE (W-7405-ENG-48), NSF (AST 97-31569, INT-9726315), the Alexander von Humboldt Foundation (FLF-1065004), and the Swiss NSF (2124-055832.98).

REFERENCES

1. S.E. Woosley and T.A. Weaver, *Ap. J. Suppl.* 101 (1995) 181.
2. F.-K. Thielemann, K. Nomoto, and M.-A. Hashimoto, *Ap. J.* 460 (1996) 408.
3. T. Rauscher, R.D. Hoffman, A. Heger, S.E. Woosley, *Ap. J.*, in prep.
4. A. Heger, K. Langanke, G. Martínez-Pinedo, S.E. Woosley, PRL, submitted.
5. J.J. Cowan, A.G.W. Cameron, and J.W. Truran, *Ap. J.* 294 (1985) 656.
6. C. Freiburghaus, et al., *Ap. J.* 516 (1999) 381.
7. K.L. Kratz, et al., *Ap. J.* 402 (1993) 216.
8. S.E. Woosley and W.M. Howard, *Ap. J. Suppl.* 36 (1978) 285.
9. M. Rayet, M. Arnould, M. Hashimoto, N. Prantzos, K. Nomoto, *A&A* 298 (1995) 517.
10. H. Nieuwenhuijzen and C. de Jager, *A&A* 231 (1990) 134.
11. C.A. Iglesias and F.J. Rogers, *Ap. J.* 464 (1996) 943.
12. N. Itoh, H. Hayashi, A. Nishikawa, and Y. Kohyama, *Ap. J. Suppl.* 102 (1996) 411.
13. T. Rauscher, F.-K. Thielemann, and K.-L. Kratz, *Phys. Rev. C* 56 (1997) 1613.
14. T. Rauscher and F.-K. Thielemann, *ADNDT* 75 (2000) 1.
15. Z. Bao, et al., *ADNDT* 76 (2000) 1.
16. Zs. Fülöp, et al., *Z. Phys. A* 355 (1996) 203.
17. E. Somorjai, et al., *A&A* 333 (1998) 1112.
18. T. Rauscher, F.-K. Thielemann, J. Görres, M. Wiescher, *NP A675* (2000) 695.
19. R.D. Hoffman, S.E. Woosley, and T.A. Weaver, *Ap. J.* (2000), submitted.
20. C. Angulo, et al., *NP A656* (1999) 3.
21. J.K. Tuli, et al., *Nuclear Wallet Cards*, 5th edition, Brookhaven National Laboratory, USA (1995); K.L. Kratz, et al., priv. comm.; F.-K. Thielemann, priv. comm.
22. P. Möller, J.R. Nix, and K.L. Kratz, *ADNDT* 66 (1997) 131.
23. D. Belic, et al., *PRL* 83 (1999) 5242.
24. K. Langanke and G. Martínez-Pinedo, *NP A673* (2000) 481.
25. M. Rayet, this volume.